Proc. Natl. Acad. Sci. USA
Vol. 78, No. 9, pp. 5564–5568, September 1981
Biophysics

Electrostatic control of the efficiency of light-induced electron transfer across membranes

(photosynthesis/light energy storage/charge separation/bioenergetics)

ARIEH WARSHEL AND DONALD W. SCHLOSSER

Department of Chemistry, University of Southern California, Los Angeles, California 90007

Communicated by Martin D. Kamen, May 5, 1981

ABSTRACT **The energetics and efficiency of light-induced electron transfer across membranes is examined on a molecular level. It is found that the activation energies that control the efficiency are determined by the solvation energies of the charge-transfer states, the redox potentials of the donors and acceptors, and the dielectric relaxation of the system. The formalism developed allows one to assess the efficiency of any artificial photosynthetic system in terms of its molecular components and their local environment. It is pointed out that the key problem in designing an efficient photosynthetic system is the transfer of a charge through a low dielectric environment and that this problem cannot be overcome by choosing the position of the primary donor and acceptor in the membrane. It is predicted that artificial photosynthetic systems can be optimized by placing the acceptors in polar sites that provide a large effective dielectric constant and low dielectric relaxation and by arranging the acceptors in order of increasing redox potentials. The implication regarding bacterial photosynthesis is discussed.**

Photosynthesis is the most efficient known process for conversion and storage of light energy. Photosynthetic systems operate by light-induced charge separation across membranes where the electrostatic energy of the charge-separated state is stored in the form of a pH gradient accompanied by conversion of ADP to ATP (e.g., see ref. 1). Understanding the microscopic factors that determine the efficiency of such systems is one of the most fundamental problems in photobiology and the key bottleneck in designing artificial photosynthetic membranes. The efficiency of photosynthetic systems has been analyzed from phenomenological thermodynamic considerations (2–4), but no attempt has been made to define the microscopic requirements for efficient photosynthesis or to relate the energetics of light-induced charge separation across membranes to the local dielectric environment and molecular components involved. It is clear that nature has achieved efficient photosynthesis by building an optimally arranged protein–membrane system. It is not clear, however, what the problems are that were solved. To address this issue, we take the engineering approach and examine specific problems in developing an efficient conduction chain for light-induced electron transfer across membranes. We find that the overall efficiency can be expressed in terms of the stabilization (solvation) of the charge-transfer states by their local dielectric environment, the oxidation and reduction potentials of the donors and acceptors, and the dielectric relaxation at their sites. It is shown that the key problem faced by a designer (and by evolution) is the inherent barrier of transferring charge through the low dielectric region of the membrane.

The publication costs of this article were defrayed in part by page charge payment. This article must therefore be hereby marked "*advertisement*" in accordance with 18 U. S. C. §1734 solely to indicate this fact.

Phenomenological considerations of photosynthetic efficiency

Photosynthetic units that transfer charge across membranes can be described schematically as conduction chains (Fig. 1). The overall process of light-induced charge separation by such systems can be represented in a phenomenological way by diagrams of the type presented in Fig. 2. This figure shows how absorption of light by the ground state, 0, forms an excited state, 1, that relaxes to the initial charge-transfer state, 2. State 2 can either relax to state n by further charge separation or return to ground state 0. The efficiency of energy storage for absorbed photons can be defined as

$$\eta(\tau) = C_n(\tau)\,\Delta G_{0\to n}/\Delta G_{0\to 1}, \qquad [1]$$

where $\Delta G_{0\to 1}$ and $\Delta G_{0\to n}$ are the free energies of the initial exciton state and the final charge-transfer state, respectively. $C_n(\tau)$ is the fraction of molecules in state n at a time, τ, characteristic of converting the charge-separation energy of state n to other forms of energy (e.g., τ^{-1} can be the rate of conversion of ADP to ATP).

For the system described by Eq. 1, it is possible to show from kinetic considerations (5) that the population of state n as a function of time is approximately

$$C_n(t) \cong \phi\, Y_n[\exp(-\bar{k}_2 t) - \exp(-\bar{k}_1 t)], \qquad [2]$$

where ϕ is the quantum yield of populating state 2 ($\phi = k_{1\to 2}/(k_{1\to 0} + k_{1\to 2})$ in which $k_{1\to 0}$ is the rate of fluorescence and radiationless transitions from state 1 to state 2. The yield of populating state n from state 2 is given by $Y_n = k_{2\to n}/(k_{2\to n} + k_{2\to 0} + k_{n\to 2})$. The rate at which state n is populated from state 2 is given by $\bar{k}_1 = k_{2\to n} + k_{2\to 0} + k_{n\to 2}$, and the rate at which the population of state n decays is given by $\bar{k}_2 = k_{2\to 0}k_{n\to 2}/(k_{2\to n} + k_{2\to 0} + k_{n\to 2})$. Eq. 2 was derived under the assumption that $k^2_{2\to n} > k_{2\to 0}\,k_{n\to 2}$, which is satisfied by systems with significant efficiency. For an efficient system, the parameters defining $C_n(\tau)$ must assume values of $\phi \cong 1$, $Y_n \cong 1$, and $\bar{k}_2\tau < 1$. These constraints are of phenomenological nature and do not reveal the molecular constraints imposed on the efficiency of the conduction chain.

Understanding the microscopic basis for efficiency requires analysis of the individual rate constants, $k_{i\to j}$, in terms of the corresponding activation energies $\Delta G^{\ddagger}_{i\to j}$:

$$k_{i\to j} = B_{i\to j} \exp\{-\Delta G^{\ddagger}_{i\to j}/RT\}. \qquad [3]$$

In the next section, the activation energies are related to a microscopic model of electron transfer across membrane.

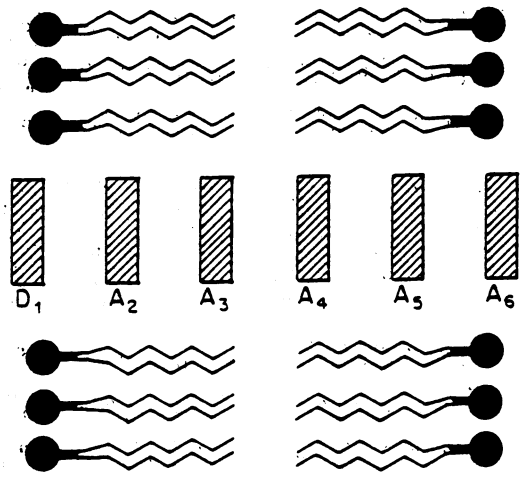

FIG. 1. A schematic model of a conduction chain for light-induced charge separation across membrane. The chain is composed of a donor (D_1) and acceptors (A_i) that span the width of the membrane.

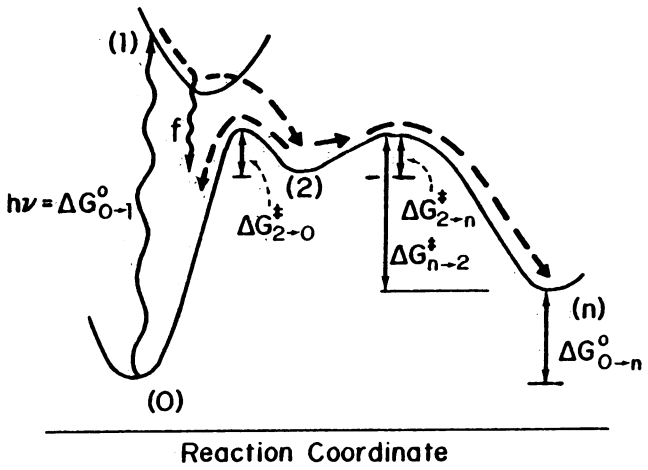

FIG. 2. A phenomenological description of the energetics of light-induced charge separation.

Energetics and dynamics of charge separation across membranes

In this section, we derive the effective rates of light-induced charge separation in terms of the microscopic parameters of the system. As an example, we will use the conduction chain of Fig. 1. The same type of treatment can be applied to other configurations (e.g., D in the middle of the membrane). Light-induced charge separation in the system of Fig. 1 can be represented as (5).

$$D_1^0A_2^0A_3^0 \dots A_n^0 \rightleftharpoons D_1^*A_2^0A_3^0 \dots A_n^0 \rightleftharpoons D_1^+A_2^-A_3^0 \dots A_n^0 \rightleftharpoons \dots \rightleftharpoons D_1^+A_2^0A_3^0 \dots A_n^- , \quad [4]$$

where 0 and * indicate ground and excited states, respectively, and we neglect all transitions except these that involve hopping of only one charge [(+) or (−)] between neighboring sites.† The successive stages of Eq. 4 will be denoted:

$$(0) \rightleftharpoons (1) \rightleftharpoons (2) \rightleftharpoons \dots \rightleftharpoons (n), \quad [5]$$

where $D_1^+A_2^0 \dots A_j^- \dots A_n^0$ or $D_1^+A_j^-$ is denoted as (j). The parameters defining the rate constants of Eq. 3 can be expressed by a formula that includes a classical term for the low-frequency modes (6, 7) and a quantum mechanical term for tunneling through the high-frequency modes (8, 9):

$$B_{i\to j} \simeq (2\pi\sigma^2/\hbar)(4\pi\alpha RT)^{-1/2} \exp[-S_r]. \quad [6]$$

$$\Delta G^{\ddagger}_{i\to j} \simeq [\Delta G^0_{i\to j} \pm (-n_r hc\bar{\nu}_r) + \alpha]^2/(4\alpha) + (n_r \pm n_r)hc\bar{\nu}_r/2 - RT \ln(S_r^{n_r}/n_r!),$$

where $i \to j$ denotes $D_1^+A_i^- \to D_1^+A_j^-$, σ is the Hamiltonian matrix element between $A_i^-A_j^0$ and $A_i^0A_j^-$, $\Delta G^0_{i\to j}$ is the difference between the equilibrium free energies§ of the $A_i^-A_j^0$ and $A_i^0A_j^-$ systems, and the $(\pm)$ signs are for positive and negative $\Delta G^0_{i\to j}$, respectively. As shown in Fig. 3, α is the change in energy of the $A_i^0A_j^-$ system when its coordinates are displaced from their equilibrium position to that of the $A_i^-A_j^0$ system. However, α does not include the effect of displacements along high-frequency modes, which are represented here by a single effective frequency (in cm^{-1}), $\bar{\nu}_r$. S_r is proportional to the square of the dimensionless displacement corresponding to the frequency $\bar{\nu}_r$ and takes values of approximately 0.7 in typical chromophores (9). n_r is the quantum number of the effective mode $\bar{\nu}_r$ that minimizes $\Delta G^{\ddagger}$.

The classical expression for the activation energy, $\Delta G^{\ddagger}$, which is given by Eq. 6 with $n_r = 0$, is valid when the size of α is larger than that of $\Delta G^0_{i\to j}$ (Fig. 3*a*). When the size of α is less than that of $\Delta G^0_{i\to j}$ (Fig. 3*b*), the classical expression greatly overestimates the realistic barrier to electron transfer from i to j, and the effects of tunneling through quantum modes must be included. The effect of tunneling is taken into acount by varying the quantum number n_r in Eq. 6 until the minimum $\Delta G^{\ddagger}_{i\to j}$ is found. In a study of bacterial photosynthesis (9), it was found that the neglect of tunneling in the $2 \to 0$ reaction leads to errors of more than 10 orders of magnitude in the calculated rate. It appears that the importance of the $n_r \neq 0$ channels in electron-transfer processes has been overlooked by many workers in this field.

For an arrangement of stacked acceptors, the rate constants and, therefore, the overall efficiency can be analyzed by using Eqs. 3 and 6 in terms of the $\Delta G^0_{i\to j}$s, αs and $B_{i\to j}$s as described in the next sections.

The Electrostatic Control of $\Delta G^0_{i\to j}$. This section analyses the $\Delta G^0_{i\to j}$ for the various charge-transfer states and shows how the solvation energies and redox potentials can be used to provide a rough estimate of the energetics of the overall charge-sepa-

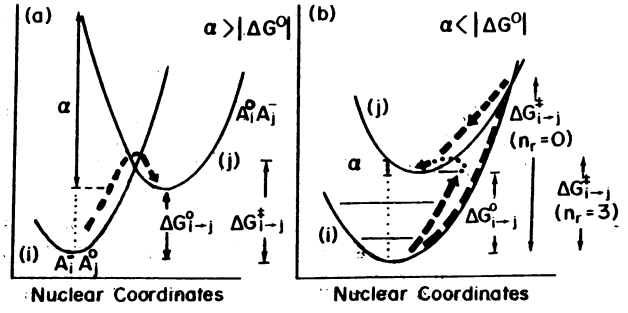

FIG. 3. The relation between ΔG^0, α, and $\Delta G^{\ddagger}$ in electron-transfer reactions. For $\alpha < |\Delta G^0|$, the figure shows an alternative channel of tunneling (·····) that reduces the activation energy.

† Hopping between nonneighboring sites could be important when other channels of electron transfer are closed.

§ In a realistic multidimensional system, the energy difference in Eq. 6 should be taken as a difference in free energy rather than a difference in potential energy (unpublished data). The ΔGs in this work are considered concentration-independent standard free energies.

ration process. The formalism developed previously for analyzing the energetics of the proton pump of bacteriorhodropsin in (10) is used. In this formalism the free energy of the $A_i^+A_j^-$ charge-transfer state (relative to that of the uncharged ground state) is given by

$$\Delta G^0_{0\to A_i^+A_j^-} = \Delta G^i_{sol} + \Delta G^j_{sol} - 1/r_{ij}\,\varepsilon_{ij} + \Delta I^w_{i+} + \Delta I^w_{j-}, \quad [7]$$

where ΔG^i_{sol} is the change in solvation energy of the ith group upon transfer from solution to its site in the membrane, r_{ij} is the distance between i and j, ε_{ij} is the distance-dependent dielectric constant (defined in ref. 10), and $\Delta I^w_{i,q}$ is the free energy of forming the charged form of the ith group from its uncharged form in solution. The ΔIs are obtained from the redox potentials of the corresponding groups in solution. Eq. 7 expresses the work ($\Delta I^w_{i+} + \Delta I^w_{j-}$) for forming the charged ith and jth groups in aqueous solution at infinite separation and the electrostatic work of bringing the two charged groups to their respective sites in the membrane. With this expression, we can evaluate the ΔG^0 for different types of conduction chains.

For a conduction chain of identical acceptors placed inside a membrane in a region of low dielectric ($\varepsilon = 2$), where D_1 is placed in aqueous solution, $\Delta G^1_{sol} \cong 0$ (because D_1 is in water) and $\Delta G^j_{sol} - 1/(r_{1j}\varepsilon_{1j})$ is given to a good approximation by ΔG^j_{sol}. Thus, we can express the energy of the jth charge-transfer state relative to the final state, n, (where both charges are in aqueous solution) by the energy of taking the jth charged group from solution to its site in the membrane. The contribution of ΔG^j_{sol} can be estimated by considering the membrane and the solution as continua with dielectric constants 2 and 80, respectively. The energy of the charge jth group relative to its energy in solution is given (in kcal/mol) by (5)

$$\Delta G^j_{sol} \cong 83\{1/\bar{a} - 1/(4R_j) - 1/[4(L - R_j)]\}, \quad [8]$$

where $\bar{a}$ is the effective radius of the acceptor in Å, L is the width of the membrane, and R_j is the distance of the jth group from the membrane boundary. The dependence of ΔG^j_{sol} on R_j is shown in Fig. 4. The value of the ΔG^j_{sol} curve at R_2 determines the energy of state 2 for the given value of $\Delta I^w_1 + \Delta I^w_2$. The values obtained from the figure provide simple lower limits for the crucial activation energies $\Delta G^{\ddagger}_{2\to n}$ and $\Delta G^{\ddagger}_{n\to 2}$. For example, in the situation presented in Fig. 4, $\Delta G^0_{2\to 4}$ and $\Delta G^0_{n\to 4}$ are the lower limits for $\Delta G^{\ddagger}_{2\to n}$ and $\Delta G^{\ddagger}_{n\to 2}$, respectively. Although a more refined treatment requires the exact evaluation of the activation energies (using Eq. 6), the rough lower limit provided by Eq. 8 is sufficient in many cases for estimating the efficiency of a given system.

α in Various Dielectrics. There are two contributions to the energy relaxation α: an intramolecular contribution, α_0, due to the change in the geometry of the donor and acceptor along the low-frequency modes [the effective α_0 is about 1 kcal/mol for typical aromatic molecules at room temperature (5, 9)] and an intermolecular contribution, $\alpha(\varepsilon)$, due to relaxation of the surrounding solvent and changes in the distances between neighboring acceptors (9). In the case of a donor and acceptor that are embedded in the same dielectric and separated by a distance $\bar{X}$, the solvent contribution to $\alpha(\varepsilon)$ is given (in kcal/mol; ref. 6) by

$$\alpha(\varepsilon) = 322\,(1/\bar{a} - 1/\bar{X})(\varepsilon - 2)/(2\varepsilon). \quad [9]$$

Note that when $\varepsilon = 2$, $\alpha(\varepsilon) = 0$.

For a case in which the donor is in an environment with $\varepsilon = 80$, the acceptor in an environment with $\varepsilon = 2$, and $\bar{X}$ is larger than $2\bar{a}$, we obtain (from considerations similar to that of ref. 6)

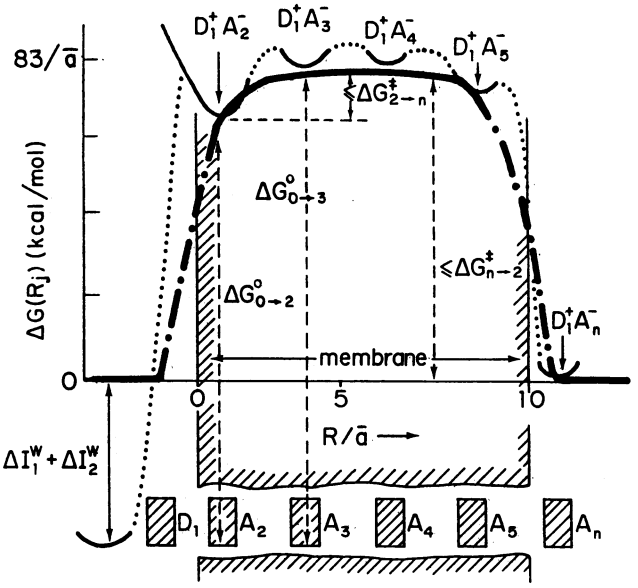

FIG. 4. Evaluating the ΔG^0s for light-induced electron transfer in the system of Fig. 1. ——, Evaluation with Eq. 8; –·–, a more realistic interpolation requiring that ΔG will vanish at $R = -\bar{a}$. The energy of the jth state is simply determined by the value of the ΔG^0 curve at the position of A_j. The lower limit of the activation energy $\Delta G^{\ddagger}_{2\to n}$ is determined by the difference between the maximum of ΔG^0 and the energy of state 2.

$$\alpha(\varepsilon_1 = 2, \varepsilon_2 = 80) \cong 166/(2\bar{a}). \quad [10]$$

$B_{i\to j}$. The preexponential factor, $B_{i\to j}$, at room temperature can be expressed approximately (in sec^{-1}; ref. 5) by

$$B_{i\to j} \cong \theta^2\, 10^{12}\exp[-2.7(X_{ij} - 4.6)], \quad [11]$$

where X_{ij} is the distance between the donor and acceptor and θ is an orientation factor. [θ is unity for electron transfer be-

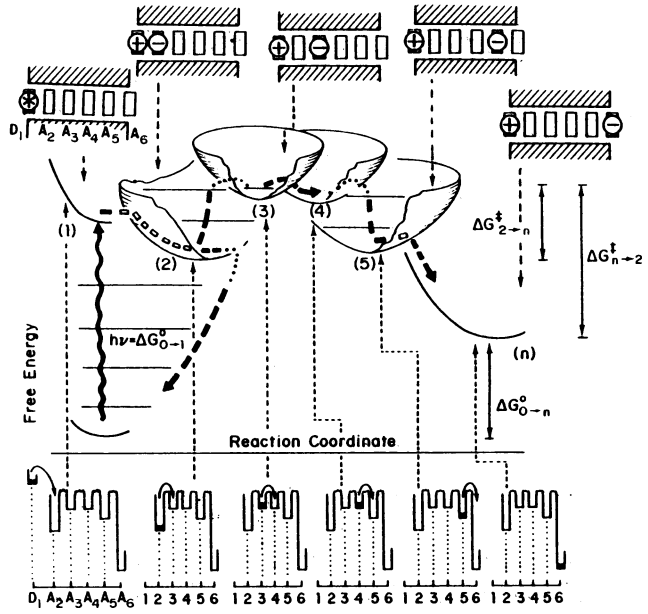

FIG. 5. The energetics and dynamics of light-induced charge separation in the conduction chain of Fig. 1. The energies of the various charge-transfer states are determined by the considerations of the first section. The positions of the charges are indicated in the diagram in the upper part of the figure.

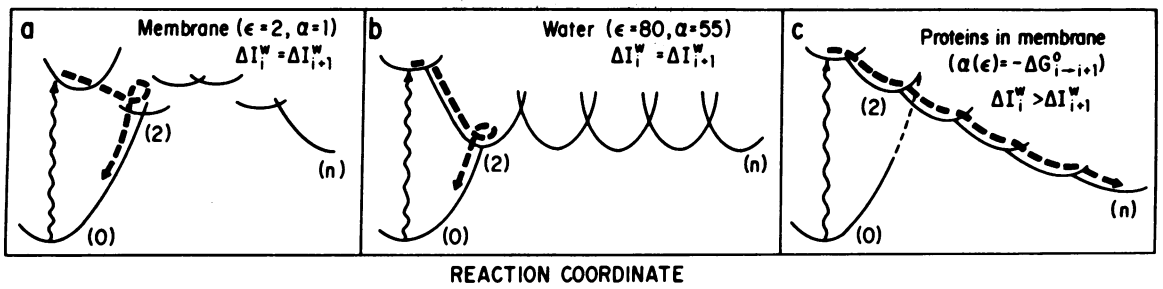

FIG. 6. Energetics and dynamics of conduction chains in several limiting cases. (*a*) A conduction chain of identical acceptors in a low dielectric membrane. This system cannot give an efficient charge separation because of the large energy of transferring the charge through the membrane. (*b*) A conduction chain of identical acceptors in aqueous solution. This is an inefficient system because of the high-activation barriers in the individual $i \rightarrow i+1$ steps. (*c*) An conduction chain that combines dielectric stabilization, redox gradient, and optimal relaxation [$\alpha(\varepsilon) = \Delta G_{i\rightarrow i+1}$]. This provides an optimal downhill charge-separation process.

tween identical molecules in parallel orientation and up to 2 orders of magnitude smaller for orthogonal orbitals, such as π^* of donor and π of acceptor, when a reasonable motion of the donor and acceptor is taken into account (9).] Because efficient population of state 2 requires that ϕ in Eq. 2 is close to unity, $k_{1\rightarrow 2}$ must be larger than $k_{1\rightarrow 0}$, which is of the order of 10^9 sec^{-1} in typical conjugated molecules. This requires from Eq. 11 that X_{12} is smaller than 5 Å. The constraints on the distances between other acceptors are less severe, and we assume for all i larger than one average values of $\bar{X} = X_{i,i+1}$ and $\bar{B} = B_{i\rightarrow i+1} = B_{i+1\rightarrow i}$.

Optimization of the efficiency of conduction chains

In this section, the efficiency of conduction chains is examined in terms of the microscopic parameters developed in the previous section.

As a simple example, we consider the system shown in Fig. 1 and calculate the efficiency of a conduction chain of identical acceptors ($\Delta I_i^w = \Delta I_{i+1}^w$) embedded in a membrane with a uniform dielectric constant of $\varepsilon = 2$. The free energies of the charge-separation process for this system is shown schematically in Figs. 5 and 6*a*. By assuming an effective radius of the acceptors[¶] of $\bar{a} = 3$ Å and that D_1 is in solution ($R_1 \leq -3$ Å) and by using the requirement that X_{12} is less than 5 Å (which requires $R_2 \leq 2$ Å), Eq. 8 gives $\Delta G^0_{2\rightarrow 3} = \Delta G^3_{sol} - \Delta G^2_{sol} \simeq 10$ kcal/mol. From Eq. 6, the activation energy of the forward reaction for the situation shown in Fig. 5 is given by $\Delta G^{\ddagger}_{2\rightarrow n} \cong \Delta G^{\ddagger}_{2\rightarrow 3} \cong 11$ kcal/mol. By using a typical value of $\Delta I_1^w + \Delta I_2^w$ of 40 kcal/mol, value for $\Delta G^{\ddagger}_{2\rightarrow 0}$ of 4 kcal/mol is found. With $B_{2\rightarrow 0} = \bar{B}$, the efficiency of this system cannot exceed 6×10^{-6}. Even if $\bar{B}$ is 2 orders of magnitude larger than $B_{2\rightarrow 0}$, the efficiency of the system is small. The reason for the inefficiency is the relatively high activation barrier associated with transfer of a charge through a low dielectric region. It can be shown (5) that the same or higher "dielectric barrier" exists in other conduction chains of molecules with similar ΔI^w, including the cases when the primary donor and acceptor are placed in the middle of the membrane or when D_1 is on the membrane boundary ($R_1 = 0$).

To understand how nature overcomes the problems inherent in light-induced charge separation across a membrane of low dielectric, we examine the conditions for maximum efficiency in Eq. 2. The optimal value of $C_n(\tau)$ is obtained with $Y_n \cong 1$, $k_2\tau < 1$ and $\phi \cong 1$. The first two constraints are satisfied (5) when

$$0 \cong \Delta G^{\ddagger}_{2\rightarrow n} < \Delta G^{\ddagger}_{2\rightarrow 0} + RT \ln(\bar{B}/B_{2\rightarrow 0}), \quad [12]$$

$$0 < \Delta G^0_{n\rightarrow 2}, \quad [13]$$

$$\Delta G^0_{n\rightarrow 2} + \Delta G^{\ddagger}_{2\rightarrow 0} > RT \ln(B_{2\rightarrow 0}\tau), \quad [14]$$

in which the condition $\Delta G^{\ddagger}_{2\rightarrow 0} > 0$ is satisfied in most conceivable conduction chains (5). The constraint $\phi \cong 1$ provides no insight into the dielectric control of the overall process. It can be satisfied as long as X_{12} is less than 5 Å (Section II) by choosing a primary donor and acceptor that give a value of $\Delta G^0_{1\rightarrow 2}$ such that $\Delta G^{\ddagger}_{1\rightarrow 2} = 0$ (5). Our main interest in this work is in the ways to satisfy the conditions of Eqs. 12, 13, and 14. The main options are the following.

(*i*) Active Site Polarity. As shown in Fig. 4, the condition that $\Delta G^{\ddagger}_{2\rightarrow n} \cong 0$ is difficult to satisfy in a simple conduction chain in a membrane with a low dielectric environment because ΔG_{sol} increases drastically with increasing charge separation (see first section), which gives a large activation energy for the $2 \rightarrow 3$ reaction. Biological systems can overcome this problem and reduce ΔG_{sol} to 0 by placing the acceptors in protein active sites, where the charged form of the acceptors will be stabilized by permanent dipoles (e.g., hydrogen bonds) of the protein (11). However, as shown in Fig. 6*b*, the condition $\Delta G_{sol} \simeq 0$ is still not sufficient for efficiency when $\Delta I^i_w = \Delta I^w_{i+1}$ because $\Delta G^0_{2\rightarrow n} \simeq \Delta G^0_{n\rightarrow 2} \simeq 0$ and Eq. 13 is not satisfied.

(*ii*) Redox Gradient. Eq. 13 can be satisfied when $\Delta G_{sol} \simeq 0$ by choosing acceptors so that they are arranged in a "redox gradient" with $\Delta I_i^w > \Delta I_{i+1}^w$, where the free energy of the backwards reaction, $\Delta G^0_{n\rightarrow 2}$, satisfies Eq. 14. The $\Delta G^0_{i\rightarrow i+1}$s will then be negative (as in Fig. 6*c*). Note that the optimal value of $\Delta I^w_{i+1} - \Delta I^w_i$ depends on the corresponding values of ΔG_{sol}.‖

(*iii*) Optimal Relaxation. Given $\Delta G^0_{i\rightarrow i+1}$, the only additional condition for optimal efficiency is the choice of α. As was pointed out above, α has two contributions: $\alpha_0 \simeq 1$ kcal/mol and an $\alpha(\varepsilon)$ that depends on the dielectric relaxation of the environment and the interaction with neighboring acceptors. When $n_r = 0$, the optimal $\alpha(\varepsilon)$ that gives $\Delta G^{\ddagger}_{i\rightarrow i+1} \simeq 0$ is

$$\alpha(\varepsilon) = \Delta G^0_{i\rightarrow i+1} - \alpha_0. \quad [15]$$

The above concepts can be used as design criteria for artificial systems. To analyze the efficiency of a proposed system, the

[¶] The effective radius of a nonspherical molecule is determined by calculating the solvation energy with the microscopic model of ref. 11 and finding the radius of the spherical-charge group that gives the same solvation energy.

‖ It is well known that biological photosynthetic systems provide negative $\Delta G^0_{i\rightarrow i+1}$. However, it has not been pointed out that this gradient has two contributions: the obvious one of the ΔI^w of the prosthetic groups and the more subtle contribution of the protein dielectric stabilization to ΔG_{sol} that helps to overcome the dielectric barrier of the membrane.

$\Delta G^0_{0\to j}$s of the relevant charge-transfer states can be evaluated using Eq. 7, and the lower limits of $\Delta G^{\ddagger}_{2\to n}$ and $\Delta G^{\ddagger}_{n\to 2}$ can be obtained from diagrams such as Fig. 4. If these $\Delta G^{\ddagger}$s do not satisfy Eqs. 12–14, then the design of the system should be changed (e.g., by choosing different molecules with different ΔI^{ω}_i). Once the proper $\Delta G^0_{0\to j}$ are obtained, the deviations from Eq. 15 should be analyzed and minimized.

The photosynthetic system in bacteria operates in an efficient way that can be analyzed by the concepts of this paper. This system is described in the notation of this paper as $D_5D_1A_2A_3A_4$ in which D_5 is cytochrome *c*, D_1 is a chlorophyll dimer (or tetramer), A_2 is bacteriopheophytin, and A_3 and A_4 are ubiquinone acceptors in protein sites that probably involve bound iron. The charge separation process $D_5D^*_1A_2A_3A_4 \rightarrow D^+_5D_1A_2A_3A^-_4$ involves the separation of charges in the interior of a membrane rather than the transfer of charge from water into the membrane as discussed. The electrostatic free energy for this type of charge separation in a low dielectric environment is given in ref. 5 and involves a high activation barrier. As before, the simplest way to eliminate this barrier is by a combination of (*i*) stabilization of the acceptors by the dipoles of the protein active site to give a small value for $\Delta G_{sol} - 1/r_{ij}\varepsilon_{ij}$ and (*ii*) a redox gradient. The efficient operation of the system requires a negative $\Delta G^0_{i\to i+1}$, which is apparently satisfied (e.g., see figure 1 of ref. 12), and optimal αs. The optimal αs and their relation to protein relaxation are discussed in detail in ref. 12. We only mention here that if the primary acceptor is a tetramer rather than a monomer, then no protein relaxation is needed (12).

Discussion

The idea that photosynthetic systems operate by charge separation across membranes has been around for a long time (e.g., see ref. 13), and various aspects of light-induced electron transfer have been analyzed (9, 14). However, the crucial role of the dielectric environment has not been examined on a molecular level. This work takes a microscopic approach and shows that the overall activation barrier for the photosynthetic process can be evaluated by considering the electrostatic energies of consecutive charge transfer states. The energies of the intermediate states are analyzed in terms of the free energies of transferring charge from water to different sites in the membrane and the reduction and oxidation potentials of the donors and acceptors involved [this approach is also applicable to proton pumps (10)]. This provides a microscopic basis (Fig. 4) for phenomological diagrams such as Fig. 2. Our analysis is used to demonstrate that the key problem in designing photosynthetic systems is the intrinsic barrier associated with transferring a charge through a low dielectric region surrounded on both sides by a high dielectric medium. Although this point might seem obvious, it should be noted that the relation between the well-known principle of destabilization of charges in low dielectric environments and the overall rate of light-induced electron transfer across membranes has not been pointed out. Our formalism is used to examine the ways to obtain significant efficiency. It is found that the efficiency of light-induced charge separation can be increased by several means (*i*) The electron acceptors should be placed in polar or partially polar sites (e.g., protein active sites), where the charged forms of the acceptors are stabilized by the dipoles of their local environment. (*ii*) The acceptors should be arranged in order of decreasing redox potential, thus providing a "redox gradient" that prevents the back reaction. (*iii*) The relaxation α of the acceptor sites and the other relaxing components of the conduction chain should satisfy Eq. 15, giving a value of 0 for the activation energy of the forward reaction. As shown in Fig. 6 and argued in ref. 5, the optimal α can not be obtained in low dielectric sites and weakly interacting chromophores or in sites with too large a dielectric relaxation (e.g., aqueous sites). The optimal α can be obtained by a small relaxation of the dipoles of the local environment or by relaxation in the intermolecular interactions between neighboring components of the conduction chain [e.g., the chlorophyll dimer (9)], or by both. Obviously, various arrangements that combine dielectric control and redox gradient in different ways could be expected to provide efficient photosynthetic systems. Thus, the main point of this work is not in proposing the most efficient system but in pointing out the role of the membrane barrier and in offering a way to analyze the efficiency of various conceivable models at a microscopic level. This type of analysis is expected to be particularly useful in designing the artificial photosynthetic systems.

This work was supported by Grant GM 24492 from the National Institutes of Health and by the Alfred P. Sloan Foundation. A.W. is an Alfred P. Sloan Fellow.

1. Dutton, P. L. & Prince, R. C. (1978) in *The Photosynthetic Bacteria*, ed. Clayton, R. K. & Sistrom, W. R. (Plenum, New York), pp. 525–610.
2. Knox, R. S. (1969) *Biophys. J.* **9**, 1351–1362.
3. Parson, W. W. (1978) *Photochem. Photobiol.* **28**, 389–393.
4. Ross, R. T., Anderson, R. J. & T.-L. Hsiao (1976) *Photochem. Photobiol.* **24**, 267–278.
5. Warshel, A. (1981) *Is. J. Chem.*, in press.
6. Marcus, R. A. (1964) *Annu. Rev. Phys. Chem.* **15**, 155–196.
7. Hopfield, J. J. (1974) *Proc. Natl. Acad. Sci. USA* **71**, 3640–3644.
8. Jortner, J. (1976) *J. Chem. Phys.* **64**, 4860–4867.
9. Warshel, A. (1980) *Proc. Natl. Acad. Sci. USA* **77**, 3105–3109.
10. Warshel, A. (1979) *Photochem. Photobiol.* **30**, 285–290.
11. Warshel, A. (1978) *Proc. Natl. Acad. Sci. USA* **75**, 5250–5254.
12. Warshel, A. (1981) in *Interaction Between Iron and Proteins in Oxygen and Electron Transport*, ed. Ho, C. (Elsevier N. Holland, New York), in press.
13. Gerischer, H. & Katz, J., eds. (1978) *Light-induced Charge Separation in Biology and Chemistry* (Verlag Chem. Int., New York).
14. Jortner, J. (1981) *J. Am. Chem. Soc.* **102**, 6676–6686.